Composites: Part B 72 (2015) 1–9

Contents lists available at ScienceDirect

Composites: Part B

journal homepage: www.elsevier.com/locate/compositesb

Static analyses of FGM beams by various theories and finite elements

M. Filippi [a,*], E. Carrera [a,b], A.M. Zenkour [b,c]

[a] Department of Mechanical and Aerospace Engineering, Politecnico di Torino, Italy
[b] Department of Mathematics, Faculty of Science, King Abdulaziz University, P.O. Box 80203, Jeddah 21589, Saudi Arabia
[c] Department of Mathematics, Faculty of Science, Kafrelsheikh University, Kafr El-Sheikh 33516, Egypt

ARTICLE INFO

Article history:
Received 26 September 2014
Received in revised form 10 November 2014
Accepted 2 December 2014
Available online 12 December 2014

Keywords:
A. Layered structures
B. Mechanical properties
C. Finite element analysis (FEA)

ABSTRACT

The 1D Carrera Unified Formulation (CUF) is here used to perform static analyses of functionally graded (FG) structures. The hierarchical feature of CUF allows one to automatically generate an infinite number of displacement theories that may include any kind of functions of the cross-section coordinates (x, z), among which those used to describe the variation of the mechanical properties of FG materials. The governing equations are derived by means of the Principle of Virtual Displacements in a weak form and solved by means of the Finite Element method (FEM). The equations are written in terms of "fundamental nuclei", whose forms do not depend on the used expansions. Trigonometric, polynomial, exponential and miscellaneous expansions are here used and evaluated for various structural problems. Resulting theories are assessed by considering several aspect-ratios, gradation laws, loading and boundary conditions. The results are compared with 1-, 2- and 3-D solutions both in terms of displacements and stress distributions. The comparisons confirm that the 1D CUF elements are valuable tools for the study of FG structures.

1. Introduction

Owing to their features, Functionally Graded Materials have rapidly gained great attention in many modern applications, which require the use of efficient structures able to withstand severe operating conditions. The advantages of the FGMs are basically due to the smooth variations of their mechanical properties along preferential directions, which allow one to preserve high specific stiffness avoiding the main drawbacks of the classical composites such as the stress discontinuities at the layer-interfaces and the low resistance to temperature shocks. Thus, a considerable number of researchers has proposed theories in order to properly predict the mechanical behavior of FG structures (see, for example, [1]).

For instance, Sankar [2] developed an elasticity solution based on the Euler–Bernoulli theory for simply supported FG beams subjected to sinusoidal loads. On the other hand, Zhong and Yu [3] have provided a 2D solution in terms of Airy stress function valid for cantilever beams. Interesting results have been provided for different loadings and gradation laws. Analytical approaches have been also presented in [4–8]. The theories made use of unified formulations that allowed comparisons between the classical and higher-order beam theories. In particular, the refined displacement-based models have been obtained with the use of sinusoidal and exponential functions that yielded accurate predictions of the transverse stress field. Moreover, these refined beam models were also used in the static, free-vibration [9] and stability [10] analysis of micro-beams in the modified couple stress theory framework. Recently, Shi-Rong et al. [11] expressed the deflection, the rotational angle as well as the shear force of a FGM Timoshenko beam in terms of the deflection of the corresponding Euler–Bernoulli structure. This simplified procedure has been validated through a number of static analyses carried out on FG beams with different aspect-ratios and boundary conditions. With regard to the sandwich beams with FG core, Aprete et al. [12] developed four different analytical modeling including two equivalent single-layer approaches, a higher-order theory [13] and the Fourier-Galerkin method [14]. The variation law of core Young's modulus has been assumed to be a polynomial in the thickness direction and two beams subjected to different loading conditions have been studied. Although the simplest approaches can be considered relatively accurate, the obtained results confirmed that, for a correct prediction of the strain and stress distributions in the core, the use of higher-order theories was required.

In order to avoid the limitations of the analytical approaches, various studies have been focused on the development of efficient finite elements. For instance, Chakraborty et al. [15] proposed a

* Corresponding author. Tel.: +39 011 090 6870.
E-mail addresses: matteo.filippi@polito.it (M. Filippi), erasmo.carrera@polito.it (E. Carrera), zenkour@gmail.com (A.M. Zenkour).

http://dx.doi.org/10.1016/j.compositesb.2014.12.004
1359-8368/

super-convergent beam element based on the first-order shear deformation theory for the thermoelastic study of FG beams. A similar problem has been examined by Kadoli et al. in [16], where the third-order shear deformation theory proposed by Heyliger and Reddy was used. As expected, the higher-order beam provided more accurate results in terms of both displacements and stress distributions. Moreover, Kapuria et al. [17] presented a third order zig-zag displacement theory in conjunction with the modified rule of mixture for the static and dynamic analyses of multilayered FG structures. The results were validated through interesting experiments. Lezgy-Nazargah et al. [18] carried out static and dynamic analyses on piezoelectric beams by using a refined sinus model. The results have been found in good agreement with the reference solutions for various electrical and mechanical constrained conditions. In [19], Kutiŝ et al. compared two methods of homogenization for the electro-thermal-structural analysis of FG beams, namely the multilayering and direct integration method.

The main scope of this work is to evaluate several refined beam finite elements obtained by means of the Carrera Unified Formulation (CUF). CUF was initially introduced for the development of refined plate and shell theories [20] and later extended to beam formulation [21]. CUF has been extensively used for dealing with a wide range of structural problems including, for instance, the static and dynamic analysis of composite structures [22–25], the free vibration analysis of rotors [26] and FG structures [27–29] and the study of the mechanical behavior of structures with unconventional cross-sections [30,31]. In particular, with regard to the static behavior of FG structures, the unified formulation was previously adopted by Tornabene et al.[32] and Cinefra [33], which developed refined 2D theories using the Differential Quadrature Method and the Finite Element approach, respectively. The 1D CUF theories were instead used by Giunta et al. in [34], in which a closed form solution for simply supported beams have been provided.

The main novelty of this work, whose companion paper [27] dealt with free vibration analyses, is the use of arbitrary functions in the displacement field including those that describe the variation of the material properties (for example the exponential and trigonometric functions). Thus, the solution may be easily changed according to the problem conditions, in order to reach a good accuracy with a low number of degrees of freedom. The proposed approach has allowed us to efficiently study various structures such as thin plates, and multilayered beams subjected to several loadings and boundary conditions, in which the mechanical properties varied according to generic gradation laws. The results, compared with either solutions available in literature or 3D finite element model, have revealed the valuable capabilities of the 1D CUF beams in the study of the static behavior of FG structures.

2. The Carrera Unified Formulation

The CUF states that the displacement field, $\boldsymbol{u}(x,y,z,t)$, is an expansion of generic functions, $F_\tau(x,z)$ for the vector displacement, $\boldsymbol{u}_\tau(y)$:

$$\boldsymbol{u}(x,y,z,t) = F_\tau(x,z)\boldsymbol{u}_\tau(y,t) \qquad \tau = 1,2,\ldots,T \tag{1}$$

where T is the number of terms of the expansion and, according to the generalized Einstein's notation, τ indicates summation. The main advantage of the present approach is that it considers both type and number of functions $F_\tau(x,z)$ as input parameters. Therefore, the number of higher-order theories which can be generated is theoretically infinite. In previous papers, encouraging results were obtained by using several advanced theories based on trigonometric, exponential, polynomials and miscellaneous expansions for the study of composite structures. For a thorough and clear description of the new displacement theories, the authors suggest [22,23]. An example of a displacement model which can be used is the following:

$$\begin{aligned}
u_x &= u_{x_1} + x\,u_{x_2} + z\,u_{x_3} + x^2\,u_{x_4} + xz\,u_{x_5} + z^2 + e^{\left(1\frac{x}{a}\right)}u_{x_6} + e^{\left(1\frac{z}{b}\right)}u_{x_7} \\
&\quad + \sin\left(3\frac{\pi x}{a}\right)u_{x_8} \\
u_y &= u_{y_1} + x\,u_{y_2} + z\,u_{y_3} + x^2\,u_{y_4} + xz\,u_{y_5} + z^2 + e^{1\left(\frac{x}{a}\right)}u_{y_6} + e^{\left(1\frac{z}{b}\right)}u_{y_7} \\
&\quad + \sin\left(3\frac{\pi x}{a}\right)u_{y_8} \\
u_z &= u_{z_1} + x\,u_{z_2} + z\,u_{z_3} + x^2\,u_{z_4} + xz\,u_{z_5} + z^2 + e^{\left(1\frac{x}{a}\right)}u_{z_6} + e^{\left(1\frac{z}{b}\right)}u_{z_7} \\
&\quad + \sin\left(3\frac{\pi x}{a}\right)u_{z_8}
\end{aligned}$$

Further expansions are evaluated in the results section, in which the functions that describe the variations of material properties are included. The use of the 2D polynomials $x^i z^j$ allows one to write the so-called Taylor-like expansions (i and j are positive integers). For example, the second-order displacement field is:

$$\begin{aligned}
u_x &= u_{x_1} + x\,u_{x_2} + z\,u_{x_3} + x^2\,u_{x_4} + xz\,u_{x_5} + z^2\,u_{x_6} \\
u_y &= u_{y_1} + x\,u_{y_2} + z\,u_{y_3} + x^2\,u_{y_4} + xz\,u_{y_5} + z^2\,u_{y_6} \\
u_z &= u_{z_1} + x\,u_{z_2} + z\,u_{z_3} + x^2\,u_{z_4} + xz\,u_{z_5} + z^2\,u_{z_6}
\end{aligned} \tag{2}$$

while the third-order one becomes:

$$\begin{aligned}
u_x &= u_{x_1} + x\,u_{x_2} + z\,u_{x_3} + x^2\,u_{x_4} + xz\,u_{x_5} + z^2\,u_{x_6} + x^3\,u_{x_7} + x^2z\,u_{x_8} \\
&\quad + xz^2\,u_{x_9} + z^3\,u_{x_{10}} \\
u_y &= u_{y_1} + x\,u_{y_2} + z\,u_{y_3} + x^2\,u_{y_4} + xz\,u_{y_5} + z^2\,u_{y_6} + x^3\,u_{y_7} + x^2z\,u_{y_8} \\
&\quad + xz^2\,u_{y_9} + z^3\,u_{y_{10}} \\
u_z &= u_{z_1} + x\,u_{z_2} + z\,u_{z_3} + x^2\,u_{z_4} + xz\,u_{z_5} + z^2\,u_{z_6} + x^3\,u_{z_7} + x^2z\,u_{z_8} \\
&\quad + xz^2\,u_{z_9} + z^3\,u_{z_{10}}
\end{aligned} \tag{3}$$

The Eqs. (2) and (3) are indicated as TE2 and TE3, and the numbers are the highest exponents of the expressions. A remarkable feature of these expansions is that classical beam theories are obtainable as particular cases. It should be noted that classical theories require reduced material stiffness coefficients to contrast Poisson's locking and, for this reason, for classical and first-order models Poisson's locking is corrected according to Carrera and Giunta [21].

3. The FE formulation and preliminaries

Adopting the classical Finite Element technique, it is possible to consider arbitrary shaped cross-sections and boundary conditions. The generalized displacement vector is defined as follow:

$$\boldsymbol{u}_\tau(y) = N_i(y)\mathbf{q}_{\tau i} \tag{4}$$

where $\mathbf{q}_{\tau i}$ is the nodal displacement vector:

$$\mathbf{q}_{\tau i} = \left\{ q_{u_{x_{\tau i}}} \quad q_{u_{y_{\tau i}}} \quad q_{u_{z_{\tau i}}} \right\}^T \tag{5}$$

The Lagrange shape functions N_i are listed in [21] (Section 5.2.2), for the beam elements with 2, 3 and 4 nodes. In this paper, the elements with four nodes (B4) are used and, therefore, a cubic approximation along the y axis is obtained. Both stiffness matrix and external loading vector are derived via the Principle of Virtual Displacements:

$$\delta L_{int} = \int_V (\delta\boldsymbol{\epsilon}_p^T\boldsymbol{\sigma}_p + \delta\boldsymbol{\epsilon}_n^T\boldsymbol{\sigma}_n)dV = \delta L_{ext} \tag{6}$$

where L_{int} stands for the strain energy, L_{ext} is the work of external loadings and δ stands for virtual variation. The stress, $\boldsymbol{\sigma}$, and strain, $\boldsymbol{\epsilon}$, components are grouped as follows:

$$\begin{aligned}\boldsymbol{\sigma}_p &= \{\sigma_{zz} \quad \sigma_{xx} \quad \sigma_{zx}\}^T, \qquad \boldsymbol{\epsilon}_p = \{\epsilon_{zz} \quad \epsilon_{xx} \quad \epsilon_{zx}\}^T \\ \boldsymbol{\sigma}_n &= \{\sigma_{zy} \quad \sigma_{xy} \quad \sigma_{yy}\}^T, \qquad \boldsymbol{\epsilon}_n = \{\epsilon_{zy} \quad \epsilon_{xy} \quad \epsilon_{yy}\}^T\end{aligned} \tag{7}$$

The subscript "p" stands for terms lying on the cross-section, while "n" stands for terms lying on the other planes, which are orthogonal to the cross-section. Under the hypothesis of linear analysis and linear elastic material, the strain–displacement relations and the Hooke's law are, respectively:

$$\begin{aligned}\boldsymbol{\epsilon}_p &= \boldsymbol{D_p}\boldsymbol{u} \\ \boldsymbol{\epsilon}_n &= (\boldsymbol{D_{ny}} + \boldsymbol{D_{n\Omega}})\boldsymbol{u}\end{aligned} \tag{8}$$

$$\begin{aligned}\boldsymbol{\sigma}_p &= \boldsymbol{C}_{pp}\boldsymbol{\epsilon}_p + \boldsymbol{C}_{pn}\boldsymbol{\epsilon}_n \\ \boldsymbol{\sigma}_n &= \boldsymbol{C}_{np}\boldsymbol{\epsilon}_p + \boldsymbol{C}_{nn}\boldsymbol{\epsilon}_n\end{aligned} \tag{9}$$

The differential operators $\boldsymbol{D_p}, \boldsymbol{D_{ny}}$ and $\boldsymbol{D_{n\Omega}}$ are reported in [21]. For isotropic materials, matrices $\boldsymbol{C}_{pp}, \boldsymbol{C}_{pn}$ ($=\boldsymbol{C}_{np}^T$) and $\boldsymbol{C}_{nn}$ are:

$$\begin{aligned}\boldsymbol{C}_{pp}^k &= \begin{bmatrix} \widetilde{C}_{11}^k & \widetilde{C}_{12}^k & 0 \\ \widetilde{C}_{12}^k & \widetilde{C}_{22}^k & 0 \\ 0 & 0 & \widetilde{C}_{66}^k \end{bmatrix}, \qquad \boldsymbol{C}_{pn}^k = \begin{bmatrix} 0 & 0 & \widetilde{C}_{13}^k \\ 0 & 0 & \widetilde{C}_{23}^k \\ 0 & 0 & 0 \end{bmatrix}, \\ \boldsymbol{C}_{nn}^k &= \begin{bmatrix} \widetilde{C}_{55}^k & 0 & 0 \\ 0 & \widetilde{C}_{44}^k & 0 \\ 0 & 0 & \widetilde{C}_{33} \end{bmatrix}\end{aligned} \tag{10}$$

Since Young's modulus (E) and Poisson's ratio (ν) of functionally graded materials are functions of the coordinates (x, y, z), the coefficients $\widetilde{C}_{ij}^k(x, y, z)$ vary with the position according to the following formula:

$$\widetilde{C}_{11}^k = \widetilde{C}_{22}^k = \widetilde{C}_{33}^k = \frac{E(1-\nu)}{(1+\nu)(1-2\nu)} \qquad \widetilde{C}_{44}^k = \widetilde{C}_{55}^k = \widetilde{C}_{66}^k = \frac{E}{2(1+\nu)} \tag{11}$$

$$\widetilde{C}_{12}^k = \widetilde{C}_{13}^k = \widetilde{C}_{23}^k = \frac{E\nu}{(1+\nu)(1-2\nu)} \tag{12}$$

The apex "k" refers to the generic portion of the structure, which can be made of any kind of isotropic material. Therefore, it is possible to easily analyze composite structures and non-homogeneous sections. The virtual variation of the strain energy is rewritten in a compact format using Eqs. (1), (4), (8) and (9):

$$\delta L_{int} = \delta q_{\tau i}^T \boldsymbol{K}^{ij\tau s} q_{si} \tag{13}$$

The fundamental nucleus of the stiffness matrix $\boldsymbol{K}^{ij\tau s}$ is:

$$\begin{aligned}&\boldsymbol{K}^{ij\tau s} = I_l^{ij} \lhd \left(\boldsymbol{D}_{np}^T F_\tau \boldsymbol{I}\right)\left[\widetilde{\boldsymbol{C}}_{np}^k \left(\boldsymbol{D}_p F_s \boldsymbol{I}\right) + \widetilde{\boldsymbol{C}}_{nn}^k \left(\boldsymbol{D}_{np} F_s \boldsymbol{I}\right)\right] + \\ &\left(\boldsymbol{D}_p^T F_\tau \boldsymbol{I}\right)\left[\widetilde{\boldsymbol{C}}_{pp}^k \left(\boldsymbol{D}_p F_s \boldsymbol{I}\right) + \widetilde{\boldsymbol{C}}_{pn}^k \left(\boldsymbol{D}_{np} F_s \boldsymbol{I}\right)\right] \rhd_\Omega + \\ &I_l^{ij,y} \lhd \left[\left(\boldsymbol{D}_{np}^T F_\tau \boldsymbol{I}\right)\widetilde{\boldsymbol{C}}_{nn}^k + \left(\boldsymbol{D}_p^T F_\tau \boldsymbol{I}\right)\widetilde{\boldsymbol{C}}_{pn}^k\right] F_s \rhd_\Omega \boldsymbol{I}_{\Omega y} + \\ &I_l^{i,yj} \boldsymbol{I}_{\Omega y} \lhd F_\tau \left[\widetilde{\boldsymbol{C}}_{np}^k \left(\boldsymbol{D}_p F_s \boldsymbol{I}\right) + \widetilde{\boldsymbol{C}}_{nn}^k \left(\boldsymbol{D}_{np} F_s \boldsymbol{I}\right)\right] \rhd_\Omega + \\ &I_l^{i,yj,y} \boldsymbol{I}_{\Omega y} \lhd F_\tau \widetilde{\boldsymbol{C}}_{nn}^k F_s \rhd_\Omega \boldsymbol{I}_{\Omega y}\end{aligned} \tag{14}$$

where

$$\boldsymbol{I}_{\Omega y} = \begin{bmatrix} 0 & 0 & 1 \\ 1 & 0 & 0 \\ 0 & 1 & 0 \end{bmatrix} \qquad \lhd \ldots \rhd_\Omega = \int_\Omega \ldots \, d\Omega \tag{15}$$

$$\left(I_l^{ij}, I_l^{ij,y}, I_l^{i,yj}, I_l^{i,yj,y}\right) = \int_l \left(N_i N_j, N_i N_{j,y}, N_{i,y} N_j, N_{i,y} N_{j,y}\right) dy \tag{16}$$

The variationally coherent loadings vector is derived in the case of a generic concentrated load **P**:

$$\mathbf{P} = \{P_{u_x} \; P_{u_y} \; P_{u_z}\}^T \tag{17}$$

Any other loading condition can be similarly obtained. The virtual work due to **P** is:

$$\delta L_{ext} = \mathbf{P}\delta\mathbf{u}^T \tag{18}$$

By introducing CUF and FEM approximations, the previous equation becomes:

Table 1
Expansions used in the analyses.

	E1	E2	E3	E4	E5	E6	E7	E8	E9	E10
cost	✓	✓	✓	✓	✓	✓	✓	✓	✓	✓
sx	✓	✓	✓		✓		✓	✓		
cx		✓	✓							
sz	✓	✓	✓		✓		✓	✓		
cz		✓	✓							
sd			✓							
cd			✓							
expx				✓	✓					
expz				✓	✓					
shx						✓	✓			
chx						✓	✓			
shz						✓	✓			
chz						✓	✓			
cc									✓	
cs									✓	
sc									✓	
ss									✓	
xz								✓		
z										✓

Table 2
Transverse displacement and stresses for $L/h = 10$, $\nu = 0.25$ and loading acting at z_T.

Theory	$10\bar{u}_z(L/2, z_B)$	$\bar{\sigma}_{yy}(L/2, -h/2)$	$\bar{\sigma}_{yz}(0,0)$	DOF
EBBT Ref. [34]	−4.0311	26.928	–	
FSDT Ref. [34]	−4.0959	26.928	−2.5753	
TE3 Ref. [34]	−4.0938	26.942	−4.3468	
TE7 Ref. [34]	−4.0942	26.922	−4.4527	
Ref. [36]	−4.0942	26.922	−4.4527	
EBBT	−4.0308	26.926	–	279
FSDT	−4.0955	26.926	−2.5816	279
TE3	−4.0934	26.940	−4.3530	930
TE7	−4.0938	26.920	−4.4588	3348
E2-5_2	−4.0938	26.922	−4.4587	2418
E10-4_2	−4.0938	26.923	−4.4583	930
E10-9_2	−4.0938	26.922	−4.4587	1395

EBBT: Euler–Bernoulli Beam Theory.
FSDT: First-order Shear Deformation Theory.
–: results not provided by the model.

Table 3
Transverse displacement and stresses for $L/h = 2.5$, $\nu = 0.3$ and loading acting at z_B.

Theory	$\bar{\sigma}_{yy}(L/2, -h/2)$	$\bar{\sigma}_{yy}(L/2, h/2)$	$\bar{\sigma}_{yzmax}$	DOF
EBBT Ref. [34]	−1.6830	8.0363	–	
FSDT Ref. [34]	−1.6830	8.0360	2.0359	
TE3 Ref. [34]	−1.8354	8.5441	1.3554	
TE8 Ref. [34]	−1.8175	8.4440	1.2822	
Ref. [37]	−1.8175	8.4440	1.2805	
EBBT	−1.6830	8.0363	–	279
FSDT	−1.6830	8.0363	2.0362	279
TE3	−1.8355	8.5445	1.3548	930
TE8	−1.8175	8.4420	1.2807	4185
E2-5_2	−1.8615	8.3784	1.2750	2418
E10-4_2	−1.8620	8.3809	1.2753	930
E10-9_2	−1.8629	8.3827	1.2750	1395

EBBT: Euler–Bernoulli Beam Theory.
FSDT: First-order Shear Deformation Theory.
–: results not provided by the model.

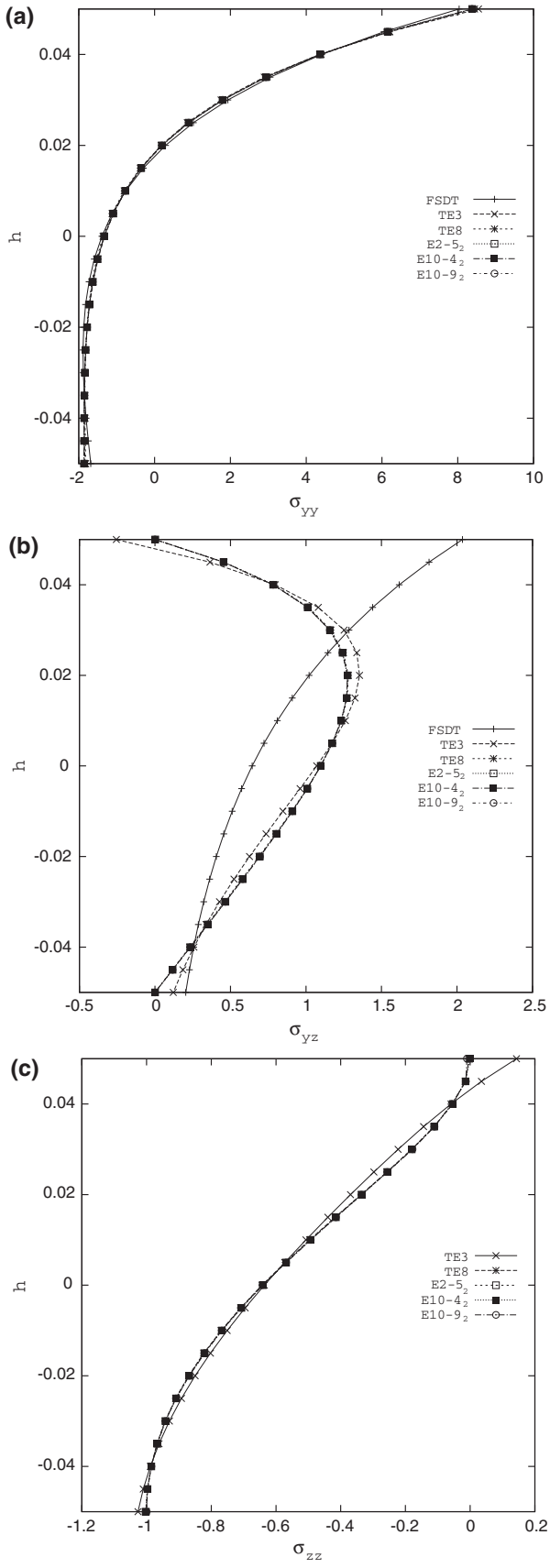

Fig. 1. Non-dimensional stress distributions through the thickness of the rectangular cross-section beam. $L/h = 2.5$.

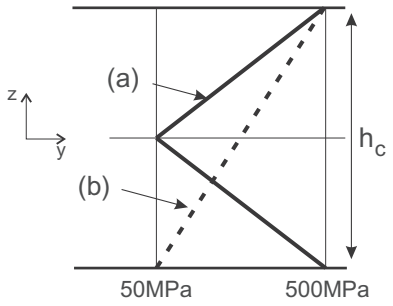

Fig. 2. Variation of E_c for sandwich beam.

$$\delta L_{ext} = F_\tau N_i \mathbf{P} \delta \mathbf{q}_{\tau i}^T \tag{19}$$

The last equation allows the identification of the components of the nucleus that have to be loaded, that is, it leads to the proper assembling of the loading vector by detecting the displacement variables that have to be loaded.

The expressions of fundamental nuclei do not vary with the approximation order of displacement theories indeed, so far, no assumption have been made on the models accuracy. In this way, it is very easy to obtain refined beam models with a completely automatic procedure.

The problem of Eq. (6) can be written in the following form:

$$\begin{aligned} &\delta \mathbf{q}^T \tilde{\mathbf{K}} \mathbf{q} = \delta \mathbf{q}^T \tilde{\mathbf{P}} \\ &\tilde{\mathbf{K}} \mathbf{q} = \tilde{\mathbf{P}} \end{aligned} \tag{20}$$

in which $\tilde{\mathbf{K}}$ and $\tilde{\mathbf{P}}$ are the global stiffness matrix and the vector of nodal forces, respectively.

4. Numerical results and discussion

4.1. Nomenclature used to denote various expansions

Although only a part of results can be shown in this section, all considered expansions are summarized in Table 1, in which acronyms are introduced. In order to understand their meaning, we may refer to the following short expressions:

- functions with single trigonometric factor:

$$sx = \sin\left(m\frac{\pi x}{a}\right) \qquad cx = \cos\left(m\frac{\pi x}{a}\right)$$
$$sz = \sin\left(n\frac{\pi z}{b}\right) \qquad cz = \cos\left(n\frac{\pi z}{b}\right)$$
$$sd = \sin\left(m\frac{\pi xz}{ab}\right) \qquad cd = \cos\left(m\frac{\pi xz}{ab}\right)$$

- functions with two trigonometric factors:

$$cc = \cos\left(m\frac{\pi x}{a}\right)\cos\left(n\frac{\pi z}{b}\right) \qquad cs = \cos\left(m\frac{\pi x}{a}\right)\sin\left(n\frac{\pi z}{b}\right)$$
$$sc = \sin\left(m\frac{\pi x}{a}\right)\cos\left(n\frac{\pi z}{b}\right) \qquad ss = \sin\left(m\frac{\pi x}{a}\right)\sin\left(n\frac{\pi z}{b}\right)$$

- hyperbolic functions:

$$chx = \cosh(mx) \qquad shx = \sinh(mx)$$
$$chz = \cosh(nz) \qquad shz = \sinh(nz)$$

- exponential functions:

$$expx = e^{(mx)} \qquad expz = e^{(nz)}$$

- polynomial functions:

$$xz = x^m z^n$$

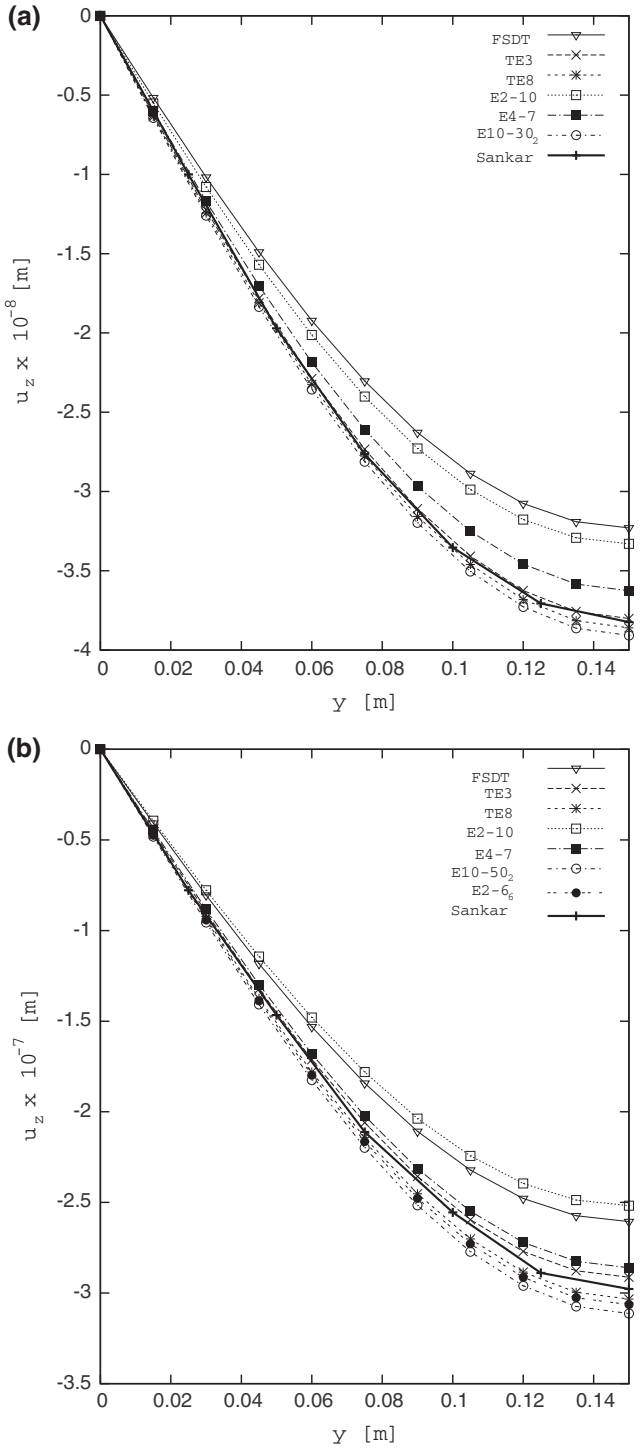

Fig. 3. Transverse displacement along the beam axis. (a): Case a; (b): Case b.

If Taylor-like expansions are added to the displacement field, their order is specified by a subscript. For example, the first component of the displacement field $E2_2$ is explicitly reported below:

$$u_x = cost\ u_{x_1} + \sin\left(\frac{\pi x}{a}\right)u_{x_2} + \cos\left(\frac{\pi x}{a}\right)u_{x_3} + \sin\left(\frac{\pi z}{b}\right)u_{x_4} + \cos\left(\frac{\pi z}{b}\right)u_{x_5} + \sin\left(2\frac{\pi x}{a}\right)u_{x_6} + \cos\left(2\frac{\pi x}{a}\right)u_{x_7} + \sin\left(2\frac{\pi z}{b}\right)u_{x_8} + \cos\left(2\frac{\pi z}{b}\right)u_{x_9} + x\,u_{x_{10}} + z\,u_{x_{11}} + x^2\,u_{x_{12}} + xz\,u_{x_{13}} + z^2\,u_{x_{14}}$$

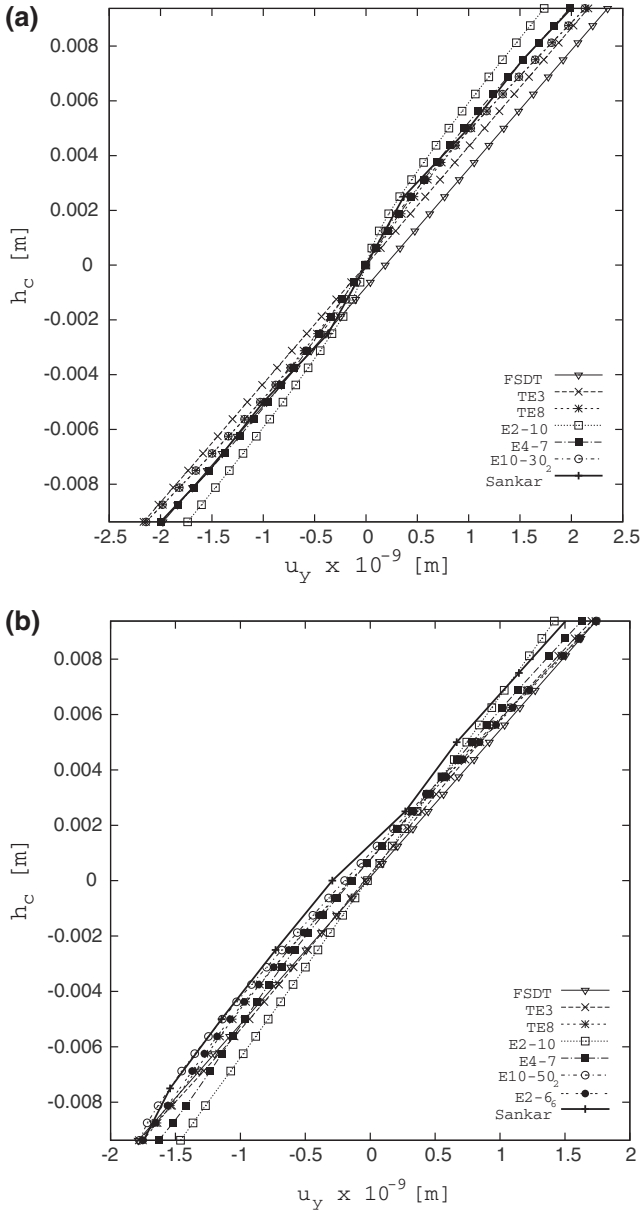

Fig. 4. Axial displacement along the core thickness. (a): Case a; (b): Case b.

As said before, the reader can refer to [22,23] for a more detailed description of the used displacement fields.

4.2. The rectangular cross-section FG beam

A rectangular cross-section beam is firstly considered in order to assess the theory. The aspect ratio of the cross-section (a/h) is assumed to be equal to 0.01 in order to neglect the effects in the width-wise direction. The structure is subjected to a sinusoidal pressure that can act either on the top (z_T) or bottom (z_B) surface, whose distribution is

$$p(x,y) = p_{zz}\,sin\left(\frac{\pi}{L}y\right) \quad p_{zz} = 1 \tag{21}$$

where 'L' is the length of the beam. The Young's modulus $E(x,z)$ varies according to the exponential law in Eq. (22) so that the ratio $E(x,z_T)/E(x,z_B)$ is equal to 10 with $E(x,z_B) = 1000$.

$$E(x,z) = E(x,z_B)\,e^{\alpha_1 x+\beta_1}\,e^{\alpha_2 z+\beta_2} \tag{22}$$

Two length-to-thickness ratios (L/h) are considered and the results are compared with those available in [34]. In their analysis, Giunta

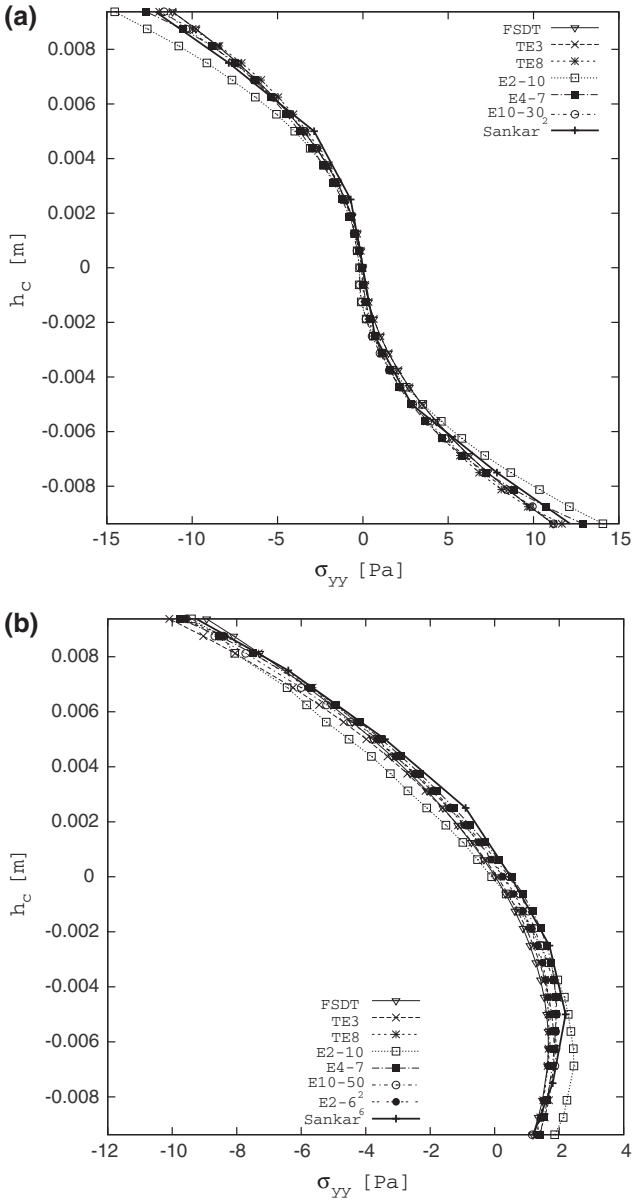

Fig. 5. Axial stresses σ_{yy} along the core thickness for various beam models. (a): Case a; (b): Case b.

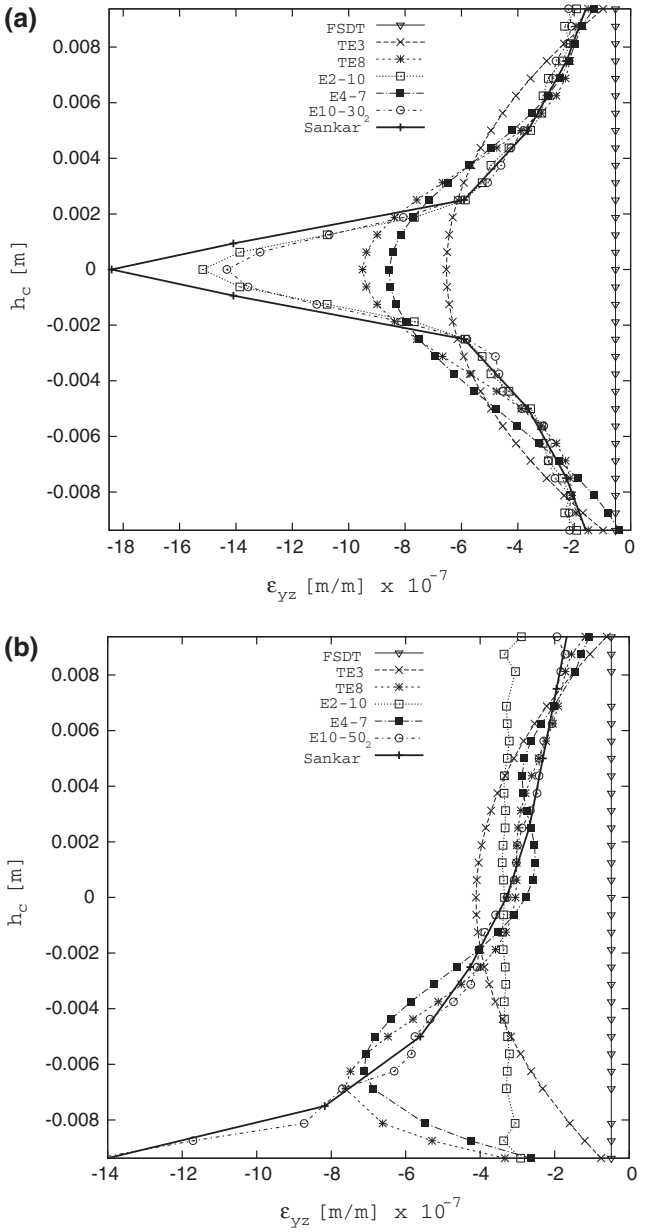

Fig. 6. Shear strain ϵ_{yz} along the core thickness for various beam models. (a): Case a; (b): Case b.

et al. provided closed form solutions using CUF, and higher-order displacement theories were obtained by adopting Taylor-type expansions: the relative results were validated by solutions available in the literature. The transverse displacement and stresses are reported in the following non-dimensional forms

$$\bar{u}_z = \frac{u_z}{h} \qquad \bar{\sigma}_{ij} = \frac{\sigma_{ij}}{p_{zz}}$$

The structure is simply supported and it is modeled using ten 4-node beam (B4) elements. Tables 2 and 3 show the results for L/h equal to 10 and 2.5, respectively. As far as classical and TE beam models are concerned, the finite element solutions agree with the analytical approach for both cases. Moreover, Fig. 1 shows the stress distributions through the thickness of the shortest beam for different displacement models. It should be noted that, for the case in point, the E10-4_2 expansion represents the best solution among the considered theories, in that it ensures the maximum accuracy both in terms of displacement and stress distributions with the lowest number of DOF.[1] This is due to the fact that the beam can be considered in a state of plane stress (in *yz*-plane), which allows to disregard the *x*-terms in the TE expansions since the transverse stresses are much more important than those along the width.

It is evident that the comparison between a number of theories makes it possible to identify the expansions that ensure a desired degree of accuracy with a certain number of DOF (usually the lowest). However, this process may be complex to undertake, in that the solutions strongly depend on the problem parameters that must be, therefore, carefully evaluated.

4.3. The sandwich structure with FG core

The refined finite elements are now used to model the simply-supported sandwich beam (L = 0.3 m) previously analyzed in [12].

[1] DOF = 3 × N_{nodes} × T, in which 'N_{nodes}' is the number of structural nodes and 'T' the number of terms in the expansion.

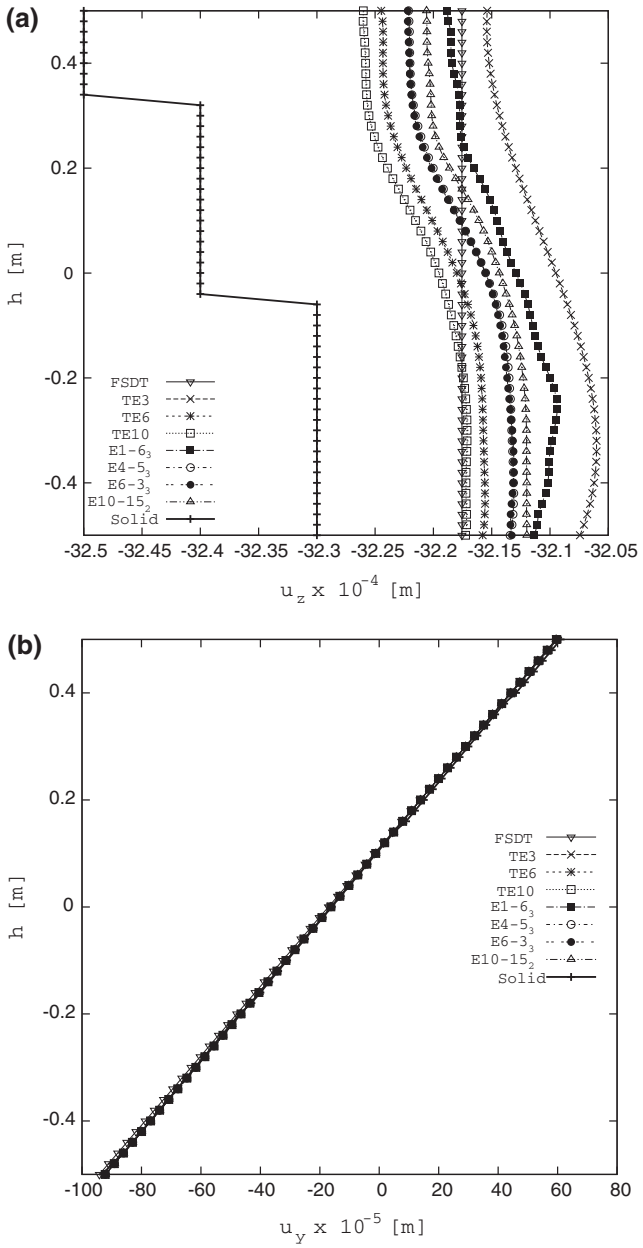

Fig. 7. Displacements along the thickness of the three-layered FG beam at $y = L$. (a): Transverse displacement; (b): Axial displacement.

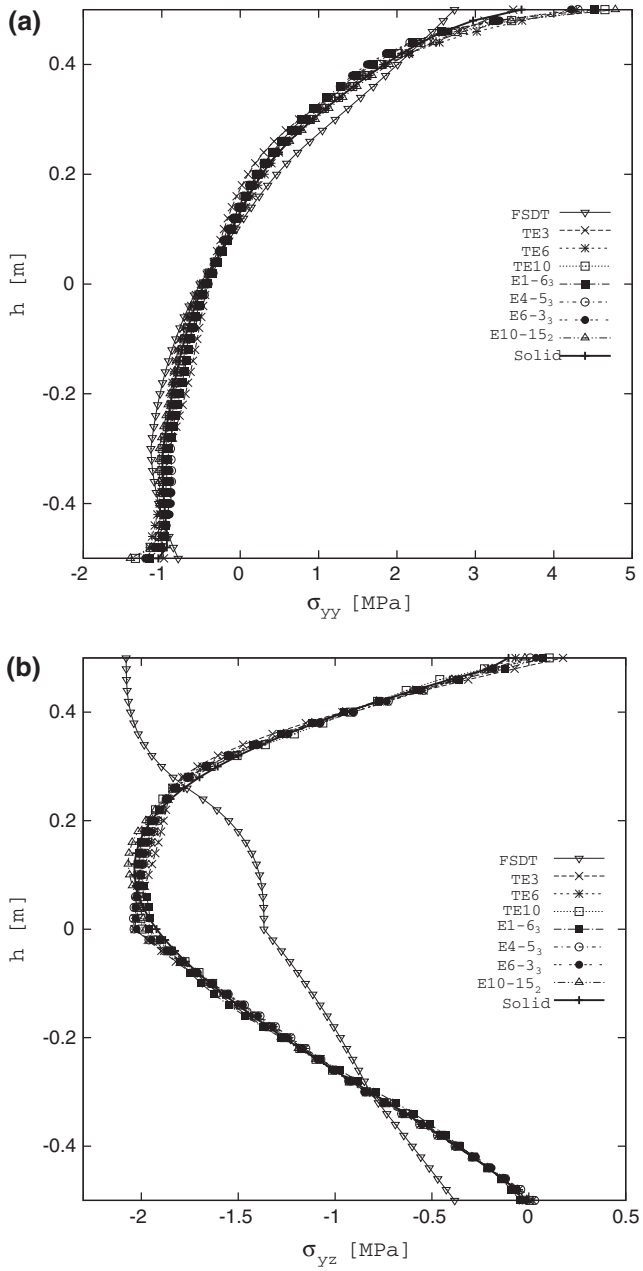

Fig. 8. Stresses along the thickness of the three-layered FG beam. (a): σ_{yy} at $y = 0$; (b): σ_{yz} at $y = 1.2$.

The core and faces thicknesses are assumed to be equal to $h_c = 0.02$ and $h_f = 0.3 \times 10^{-3}$ m, respectively. Also for this case, the width of the structure is much smaller than the other two dimensions and it is assumed to be equal to 1×10^{-4} m. Two different configurations were studied in which the variations of the Young's moduli through the core, E_c, are shown in Fig. 2 ($\nu_c = 0.35$) and the loading conditions are:

(a) : uniform pressure $p(x, y) = 1$;
(b) : sinusoidal pressure of Eq. (21).

The material of the top and bottom layers is homogeneous and isotropic ($E_f = 50$ GPa and $\nu_f = 0.25$). The results, in terms of displacements, stresses and strains, are shown in Figs. 3–6 and they are compared with the analytical solution developed by Zhu et al. [35]. The miscellaneous expansions $E10_2$ still represent the best solutions, especially for the computation of the shear strains. The Taylor-like expansions lead to accurate results only in terms of displacements and axial stresses by requiring an higher computational effort than $E10_2$ for a correct prediction of the ϵ_{yz} distributions through the thickness. The other solutions, including the FSDT, underestimate the deflections of the beams but, it is interesting to note that the E2-10 expansion gives a very accurate distribution of the shear strain for the first case. It is therefore clear that the equivalent single-layer approach can be a computationally cheap and reliable method provided that the used displacement theories may change according to the problem features.

4.4. The multi-layer FG beam

A cantilevered three-layer beam is here considered. The length 'L', the width 'a' and the whole thickness 'h' of the structure are 2.5, 0.5 and 1 m, respectively. The layers are made of functionally

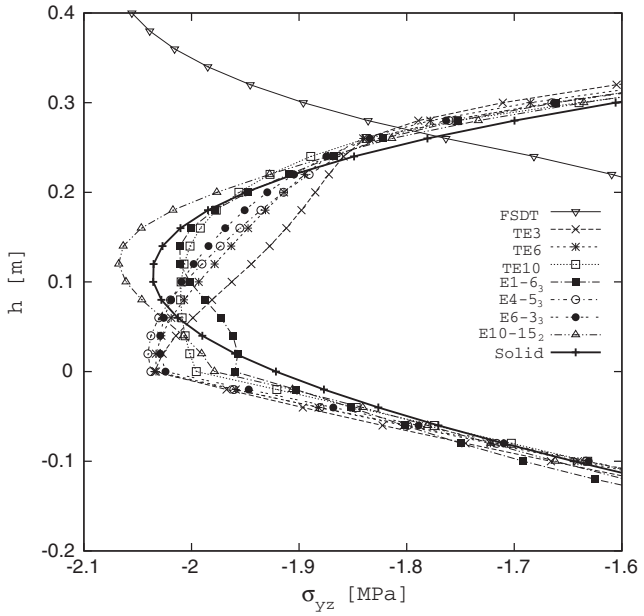

Fig. 9. Zoom of the shear stress σ_{yz} distribution along the thickness of the three-layered FG beam.

graded materials, whose Young's moduli '$E(x,z)$' follow three different gradation functions (linear, exponential and sigmoid):

$-0.5 < z < -0.3$: $E(z) = 400 \times 10^9 z + 270 \times 10^9$;
$-0.3 < z < 0.0$: $E(z) = 150 \times 10^9 \, e^{\frac{z}{0.3}\left(\ln\left(\frac{250}{150}\right)\right)+\frac{250}{150}}$;

$0.0 < z < 0.25$: $E(z) = 250 \times 10^9 V(z) + 380 \times 10^9 (1 - V(z))$ where $V(z) = 1 - \frac{1}{2}\left(1 - \frac{2(z-0.25)}{0.5}\right)^3$

$0.25 < z < 0.5$: $E(z) = 250 \times 10^9 V(z) + 380 \times 10^9 (1 - V(z))$ where $V(z) = \frac{1}{2}\left(1 + \frac{2(z-0.25)}{0.5}\right)^3$

The Poisson's ratio is considered constant and equal to 0.25 for all layers and the structure undergoes to a distributed pressure equal to 1 MPa. The beam is modeled with ten 4-node finite elements along the y-axis. For comparison purposes, a finite element solution is provided, in which solid elements HEX 8 have been used. Mechanical properties have been defined in the centroid of each element and, in order to correctly describe the materials distribution, 25, 10 and 50 elements have been used along the length, the width and the thickness, respectively. The total number of degrees of freedom of the 3D model is therefore equal to 42075. Fig. 7 show the transverse and axial displacements obtained with a number of beam theories in which polynomial, trigonometric as well as exponential functions have been used. Because of the shear effects, the transverse displacement has a non-linear variation along the thickness, and the beam results are slightly lower than the solid solution. Moreover, it is noteworthy that the FSDT predicts a constant value of u_z. The axial displacements in Fig. 7-b perfectly match the reference solution. As far as the stress distributions are concerned, it can be observed in Fig. 8 that the considered refined displacement theories lead to quite accurate results. However, slight differences of the stress distributions can be noticed in Fig. 9.

5. Conclusions

In this paper, beam finite elements based on various displacement theories was used to perform static analyses of functionally graded structures. The features of CUF allowed us to solve a number of problems considering different boundary and loading conditions, arbitrary material distributions and dimensions. The results were compared with both analytical and numerical solutions based on 2D and 3D approaches. The following remarks can be made:

- the results obtained with the Finite Element method strongly agree with the analytical beam solutions;
- although the classical beam theories provide acceptable results in terms of displacements and longitudinal stress, they do not describe the correct shear stress distributions, especially when the shear effects become relevant;
- higher-order beam theories are able to reproduce 2D results with an excellent accuracy and a low number of degrees of freedom;
- the solutions strictly depend on the problem characteristics;
- as far as the multi-layer beam is concerned, the results of the presented finite elements are close to the three-dimensional solution, which requires an higher computational effort.

The extension of 1D-CUF to the study of functionally graded structures has made it possible to solve problems which generally require bi- or three-dimensional solutions. Moreover, the dependency of the solution on the problem features proves that the $ad-hoc$ models, widely proposed in the literature, are only suitable for a limited range of analyses, therefore, the possibility to conceive a huge variety of kinematic theories appears to be a remarkable advantage of the proposed formulation. The use of a genetic algorithms could be an effective method in order to evaluate these several theories. Future works could concern the study of the temperature effects of the functionally graded materials on the dynamic properties of rotating structures.

Acknowledgements

This project was funded by the Deanship of Scientific Research (DSR), King Abdulaziz University, under Grant No. (21-130-1433-HiCi). The authors, therefore, acknowledge with thanks DSR technical and financial support.

References

[1] Swaminathan K, Naveenkumar DT, Zenkour AM, Carrera E. Stress, vibration and buckling analysis of fgm plates – a state of the art review. Compos Struct 2015:120.
[2] Sankar BV. An elasticity solution for functionally graded beams. Compos Sci Technol 2001;61:689–96.
[3] Zhong Z, Yu Tao. Analytical solution of a cantilever functionally graded beam. Compos Sci Technol 2007;67.
[4] Li X-F. A unified approach for analyzing static and dynamic behaviors of functionally graded timoshenko and eulerbernoulli beams. J Sound Vib 2008; 318.
[5] Benatta MA, Mechab I, Tounsi A, Adda Bedia EA. Static analysis of functionally graded short beams including warping and shear deformation effects. Comput Mater Sci 2008;44.
[6] Sallai BO, Tounsi A, Mechab I, Bachir Bouiadjra M, Meradjah M, Adda Bedia EA. A theoretical analysis of flexional bending of al/al$_2$o^3 s-fgm thick beams. Comput Mater Sci 2009;44.
[7] Thai HT, Vo TP. Bending and free vibration of functionally graded beams using various higher-order shear deformation beam theories. Int J Mech Sci 2012;62.
[8] Vo TP, Thai HT, Nguyen TK, Inam F, Lee J. Static behaviour of functionally graded sandwich beams using a quasi-3d theory. Composites: Part B 2015;68.
[9] Şimşek M, Reddy JN. Bending and vibration of functionally graded microbeams using a new higher order beam theory and the modified couple stress theory. Int J Eng Sci 2013;64.
[10] Şimşek M, Reddy JN. A unified higher order beam theory for buckling of a functionally graded microbeam embedded in elastic medium using modified couple stress theory. Compos Struct 2013;101.
[11] Shi-Rong L, Da-Fu C, Ze-Qing W. Bending solutions of fgm timoshenko beams from those of the homogenous eulerbernoulli beams. Appl Math Modell 2013;37.
[12] Aprete NA, Sankar BV, Ambur DR. Analytical modeling of sandwich beams with functionally graded core. J Sandwich Struct Mater 2008;10.

[13] Frostig Y, Baruch M, Vilnay O, Sheinman I. High-order theory for sandwich-beam behavior with transversely flexible core. J Eng Mech 1992;118(5):1026–43.
[14] Zhu H, Sankar BV. A combined fourier series-galerkin method for the analysis of functionally graded beams. J Appl Mech 2004;71(3):421–4. http://dx.doi.org/10.1115/1.1751184.
[15] Chakraborty A, Gopalakrishnan S, Reddy JN. A new beam nite element for the analysis of functionally graded materials. Int J Mech Sci 2003;45.
[16] Kadoli R, Akhtar K, Ganesan N. Static analysis of functionally graded beams using higher order shear deformation theory. Appl Math Modell 2008;32.
[17] Kapuria S, Bhattacharyya M, Kumar AN. Bending and free vibration response of layered functionally graded beams: a theoretical model and its experimental validation. Compos Struct 2008;82:390–402. http://dx.doi.org/10.1016/j.compstruct.2007.01.019.
[18] Lezgy-Nazargah M, Vidal P, Polit O. An efficient finite element model for static and dynamic analyses of functionally graded piezoelectric beams. Compos Struct 2013;104.
[19] Kutiš V, Murín J, Belák J, Paulech J. Beam element with spatial variation of material properties for multiphysics analysis of functionally graded materials. Comput Struct 2011;89.
[20] Carrera E. Theories and finite elements for multilayered plates and shells: a unified compact formulation with numerical assessment and benchmarking. Archives Comput Methods Eng 2003;10(3):216–96.
[21] Carrera E, Giunta G, Petrolo M. Beam structures. Classical and advanced theories. Wiley; 2011.
[22] Carrera E, Filippi M, Zappino E. Laminated beam analysis by polynomial, trigonometric, exponential and zig-zag theories. Eur J Mech – A/Solids 2013;41:58–69. http://dx.doi.org/10.1016/j.euromechsol.2013.02.006.
[23] Carrera E, Filippi M, Zappino E. Free vibration analysis of laminated beam by polynomial, trigonometric, exponential and zig-zag theories. J Compos Mater 2013. http://dx.doi.org/10.1177/0021998313497775.
[24] Ferreira AJM, Carrera E, Cinefra M, Viola E, Tornabene F, Fantuzzi N, et al. Analysis of thick isotropic and cross-ply laminated plates by generalized differential quadrature method and a unified formulation. Composites: Part B 2014;58.
[25] Ferreira AJM, Arajo AL, Neves AMA, Rodrigues JD, Carrera E, Cinefra M, et al. A finite element model using a unified formulation for the analysis of viscoelastic sandwich laminates. Composites: Part B 2012;45.
[26] Carrera E, Filippi M, Zappino E. Free vibration analysis of rotating composite blades via carrera unified formulation. Compos Struct 2013;106:317–25. http://dx.doi.org/10.1016/j.compstruct.2013.05.055.
[27] Daoud SM, Carrera E, Zenkour AM, Al Khateeb SA, Filippi M. Free vibration of fgm layered beams by various theories and finite elements. Composites: Part B 2014;59.
[28] Tornabene F, Fantuzzi N, Bacciocchi M. Free vibrations of free-form doubly-curved shells made of functionally graded materials using higher-order equivalent single layer theories. Composites: Part B 2014;67.
[29] Neves AMA, Ferreira AJM, Carrera E, Cinefra M, Roque CMC, Jorge RMN, et al. Static, free vibration and buckling analysis of isotropic and sandwich functionally graded plates using a quasi-3d higher-order shear deformation theory and a meshless technique. Composites: Part B 2013;44.
[30] Carrera E, Zappino E, Filippi M. Free vibration analysis of thin-walled cylinders reinforced with longitudinal and transversal stiffeners. J Vib Acoust 2013;135(1). http://dx.doi.org/10.1115/1.4007559.
[31] Carrera E, Petrolo M, Zappino E. Performance of cuf approach to analyze the structural behavior of slender bodies. J Struct Eng 2012;138:285–98.
[32] Tornabene F, Fantuzzi N, Viola E, Carrera E. Static analysis of doubly-curved anisotropic shells and panels using cuf approach, differential geometry and differential quadrature method. Compos Struct 2014;107.
[33] Cinefra M, Carrera E, Della Croce L, Chinosi C. Refined shell elements for the analysis of functionally graded structures. Compos Struct 2012;94.
[34] Giunta G, Belouettar S, Carrera E. Analysis of fgm beams by means of classical and advanced theories. Mech Adv Mater Struct 2010;17:622–35. http://dx.doi.org/10.1080/15376494.2010.518930.
[35] Apetre NA, Sankar BV, Ambur DR. Analytical modeling of sandwich beams with functionally graded core. J Sandwich Struct Mater 2008;10:53–74. http://dx.doi.org/10.1177/1099636207081111.
[36] Lü CF, Chen WQ, Xu RQ, Lim CW. Semi-analytical elasticity solutions for bi-directional functionally graded beams. Int J Solids Struct 2008;45:258–75. http://dx.doi.org/10.1016/j.ijsolstr.2007.07.018.
[37] Lü CF, Chen WQ, Zhong Z. Two-dimensional thermoelasticity solution for functionally graded thick beams. Sci China Ser G: Phys Mech Astronomy 2006;49:451–60. http://dx.doi.org/10.1007/s11433-006-0451-2.